

A cohesive model of dissection in arterial layers

Anna Ferrara¹, Anna Pandolfi¹

¹*Dipartimento di Ingegneria Strutturale, Politecnico di Milano, Italy*

E-mail: aferrara@stru.polimi.it, pandolfi@stru.polimi.it

Keywords: Cohesive fracture, arterial wall, dissection, finite elements.

SUMMARY. In medical terms and referring to aortic arterial damage, dissection is the separation of intra-medial tissue induced by a radial tear cutting the intima and a portion of the underlying media. Pressurized blood pervading the tear usually progresses the intramural process of dissection and may later induce formation of clots. The purpose of this study is to setup a mechanical model of arterial dissection, based on cohesive theories of fracture, able to detect the critical mechanical conditions leading to the tissue damage.

1 INTRODUCTION

The arterial wall consists of three concentric layers of a laminated-like tissue, reinforced by collagen fibers: the intima (inner layer), the media, and the adventitia (outer layer). Arterial dissection is a pathological state which refers to the separation of two layers along their interface or to the delamination within a layer of the arterial wall.

Dissections may cause narrowing of the vessel channel (stenosis) and even its entire closure, decreasing the blood flow to vital organs. Dissection also weakens the artery wall and may lead to their rupture, or to the formation of a balloon-like expansion known as aneurysm.

In the aorta, dissection is characterized by the formation of a tear in the intima. Due to the laminated structure of arterial wall, intimal tears often have sharp edges and are oriented transversally or vertically in relation to the long axis of the artery. In the dissection, the pressurized blood enters at the site of the tear and splits the middle layer (media) of the artery. Following the material laminated microstructure, the tear expands parallel to the original vessel lumen, both circumferentially and longitudinally, creating an additional passage called false lumen [1, 2]. The false lumen varies from a few millimeters to the larger classic false lumen of several centimeters, with an associated flap or septum. A combination of transverse and longitudinal dissections may produce T or cross shaped tears. In some circumstances, adjacent elastin lamellae may converge and fuse together, offering a barrier to dissection. Thus, interlamellar material and fused lamellae may prevent the initiation of dissection, or may contrast its propagation within the media [3]. Less common intramural hematoma-type dissections of the aortic wall have been identified, in which dissection is filled with blood clot without a detectable intimal tear.

Unlike aortic dissection, spontaneous coronary artery dissection is often not associated with an intimal tear. The coronaries are muscular arteries and do not contain a relevant amount of elastic laminae. The preferential surface of dissection for coronary arteries lies therefore between the adventitia and the media.

The purpose of this research is to study the process of dissection in the artery walls from the mechanical point of view, by using a finite element model, where the tissue damage is treated by using cohesive theories of fracture. The knowledge of the mechanical factors that affect and drive the arterial dissection may provide important information and useful data for the design of prevention or treatment systems. The present analyses focus on the influence of the cohesive strength and of the mesh size on the dissection evolution process. The cohesive strength, difficult to evaluate and to

measure in medical experiments, is the most important parameter controlling the dissection process.

2 THE NUMERICAL MODEL

Under physiological conditions, arteries are regarded as nearly incompressible solids. Healthy arteries behave as highly deformable composite structures and exhibit a nonlinear stress-strain response with a typical stiffening at the physiological strain level. The mechanical properties are controlled by proteins such as the rubber-like elastin and the leather-like collagen, in addition to smooth muscle cells. In the aortic media, these constituents are present in thin layers that are arranged in repeating lamellar units, each of which is about $10 \mu\text{m}$ thick and form a clear laminated structure [4]. The laminated structure confers high strength to the media and explains how the media determines the mechanical properties of the whole vessel. Unfortunately, laminated structures are prone to split, creating a cleavage plane between lamellae (dissection).

The anisotropic properties of the composite structure of the vessel walls have been evidenced in several experiments conducted in canine and porcine arteries. In particular, the arterial wall exhibits anisotropic behavior with different elastic constants in the radial, circumferential, and axial directions [7].

A few studies have been done to investigate the role of factors in the propagation of arterial dissections [5, 3, 6]. It is well known that in composite materials the failure mechanism is both related to the strength of the components and to their organization in the tissue. This is also the case of failure in structured biological tissues. The recent peeling experiments of Sommer *et al.* [8] indicated that the dissection failure response of the human aortic media is anisotropic. In the aortic media, the smooth muscle cells are oriented mostly circumferentially and may provide a more pronounced resistance to the dissection in the axial direction. In particular, the peeling in the axial direction creates a remarkably rougher dissection surface compared to that generated by peeling in the circumferential one. Contrariwise, circular-shaped dissection area obtained by an infusion technique by Carson *et al.* [3] suggest isotropic properties of the media.

In view of modeling the dissection process with finite elements, is here assumed that the material of the artery walls is hyperelastic, and the rupture of the tissues (tearing or dissection) is described through the insertion of cohesive interfaces, which account for all the tissue degenerations [15, 16, 17].

2.1 A material model for the artery walls

According to the histological evidence, in the media layer it is possible to identify two main families of fibers of equivalent stiffness and strength, inclined of a constant angle γ with respect to the circumferential direction. The resulting material structure is thus orthotropic.

Following Holzapfel *et al.* [9], the strain energy function of an anisotropic material with a double set of reinforcing fibers may be decomposed into the sum of a volumetric part Ψ_{vol} function of the volumetric deformation $J = \det \mathbf{F}$, an isotropic part Ψ_{iso} , representing the behavior of the ground matrix and of the uniformly dispersed fibers, and of an anisotropic part Ψ_{aniso} , which is totally due to the alignment of two embedded families of fibers:

$$\Psi = \Psi_{\text{vol}}(J) + \Psi_{\text{iso}}(\bar{I}_1) + \Psi_{\text{aniso}}(\bar{I}_4, \bar{I}_6), \quad (1)$$

where \bar{I}_1 is the first invariant of the modified right Cauchy-Green tensor $\bar{\mathbf{C}} = J^{-2/3} \mathbf{C}$, whereas \bar{I}_4 and \bar{I}_6 are the two pseudo-invariants measuring the square of the stretch in the direction of the fibers [10].

The expression of the strain energy functions here assumed are [17]:

$$\Psi_{\text{vol}}(J) = \frac{K}{2} \ln J, \quad (2)$$

where K is the bulk modulus of the material,

$$\Psi_{\text{iso}}(\bar{I}_1) = \frac{\mu}{2} (\bar{I}_1 - 3), \quad (3)$$

where μ is the shear modulus of the matrix, and

$$\begin{aligned} \Psi_{\text{aniso}}(\bar{I}_4, \bar{I}_6) &= \frac{k_2}{2k} \left(\exp \left[k (\bar{I}_4 - 1)^2 \right] - 1 \right) \\ &+ \frac{k_4}{2k} \left(\exp \left[k (\bar{I}_6 - 1)^2 \right] - 1 \right), \end{aligned} \quad (4)$$

where k is a dimensionless constant and k_2, k_4 are the stiffness moduli related to the collagen fiber sets. The specific form of the derived constitutive equation requires the definition of five material parameters $K, \mu, k, k_2,$ and k_4 , whose interpretations can be partially based on the underlying histological structure.

2.2 The cohesive model

Cohesive models have been used for the analysis of fracture in biological tissues [11, 12, 17]. Anisotropic (i.e. transversally isotropic) cohesive fracture has been considered in the numerical analysis of dynamic propagation of cracks by Yu *et al.* [13].

Cohesive theories see the fracture as the progressive process of separation between two surfaces originally coincident. The separation, measured as a displacement jump Δ , is resisted by cohesive tractions \mathbf{T} along the process zone, ahead of the crack tip. The experimental evidence on crack propagation, even in isotropic materials, shows that the cohesive behavior is different for opening mode (I) and sliding modes (II and III). It is therefore necessary to keep track of the orientation of the crack in order to distinguish the contribution of the normal and tangential components of the displacement jump.

In order to model the dissection process, we adopt the approach proposed by Ortiz and Pandolfi [15], combined with the automatic fragmentation procedure described in [16]. The extension to anisotropy implies the definition of: i) an anisotropic cohesive law, able to distinguish the behavior of the cohesive response along the different directions of the cohesive surface; ii) an anisotropic fracture criterion.

In cohesive theories, the displacement jump across a cohesive surface Δ plays the role of a deformation measure, while the tractions \mathbf{T} furnish the work-conjugate stress measure. In order to derive the anisotropic cohesive law, we postulate the existence of a free energy density $\Phi(\Delta)$ per unit undeformed area, that acts as a potential for the cohesive tractions, which are computed as:

$$\mathbf{T} = \frac{\partial \Phi}{\partial \Delta}. \quad (5)$$

Restricting our analysis to isothermal processes, we consider a special form of energy which depends only on the effective opening displacement δ and on one or more internal variable q (to keep track of the evolution history and account for irreversibility):

$$\Phi = \Phi(\delta, q). \quad (6)$$

with

$$\delta = \sqrt{\beta^2 [(\delta^1)^2 + \alpha^2 (\delta^2)^2] + (\delta^n)^2}, \quad (7)$$

where α and β are material parameters that account for anisotropy [15, 17].

In eq. (7) the quantities δ^i are the contravariant components of the displacement jump respect to the dual basis $\{\mathbf{m}^i\}_{i=1,2,3}$ on the cohesive surface. The covariant basis $\{\mathbf{m}_i\}_{i=1,2,3}$ is defined by the orientation of the three principal anisotropy axes $\{\mathbf{M}_i\}_{i=1,2,3}$ under change of the configuration of the body due to a motion. It is worth noting that the principal anisotropy directions define an orthonormal basis in the reference configuration, but they are described by a general basis under a generic deformation mapping. Here and in the follows, we assume $\mathbf{M}_3 = \mathbf{N}$, $\mathbf{m}_3 = \mathbf{n}$ and $\mathbf{m}^3 = \mathbf{n}$ where \mathbf{N} and \mathbf{n} are the reference and the actual normal to the cohesive surface. The differentiation of the free cohesive energy density (6) with respect to Δ_i leads to an anisotropic cohesive law of the form:

$$\mathbf{T} = \frac{\partial \Phi}{\partial \delta} \frac{\partial \delta}{\partial \Delta} = \frac{t}{\delta} [\beta^2 (\mathbf{m}^1 \otimes \mathbf{m}^1 + \alpha^2 \mathbf{m}^2 \otimes \mathbf{m}^2) + \mathbf{n} \otimes \mathbf{n}] \Delta. \quad (8)$$

In order to define an anisotropic fracture criterion, we notice that the orthotropic structure of the material assigns a different resistance to each direction. Thus, we generalize the anisotropic model used in Yu *et al.* [13] and introduce an ellipsoidal resistance surface, see Figure 1. At each

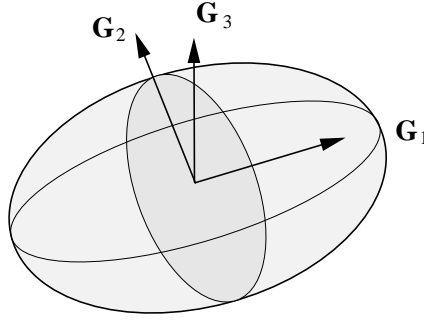


Figure 1: Resistance surface in the reference configuration. The minimum resistance is on the direction normal to the fiber plane, \mathbf{G}_3 .

principal material direction is associated in general a different tensile resistance, i.e. $\sigma_{c1} \geq \sigma_{c2} \geq \sigma_{c3}$. We assume that the corresponding critical energy release rates are $G_{c1} \geq G_{c2} \geq G_{c3}$. The material resistance $\sigma_c(\mathbf{N})$ in the direction \mathbf{N} is given by the solution of the system that represents the intersection of such direction \mathbf{N} and the resistance ellipsoid. It can be expressed as [17]:

$$\sigma_c(\mathbf{N}) = \left[\frac{M_1^2}{\sigma_{c1}^2} + \frac{M_2^2}{\sigma_{c2}^2} + \frac{M_3^2}{\sigma_{c3}^2} \right]^{-1/2}. \quad (9)$$

The test concerning the insertion of a cohesive surface is performed at the end of each loading step. At every interelement surface, an “effective” traction T is computed and compared with the material resistance associated to the normal:

$$T = \sqrt{(T^n)^2 + \beta^{-2} [(T^1)^2 + \alpha^{-2} (T^2)^2]} \leq \sigma_c(\mathbf{N}) \quad (10)$$

If the criterion is violated, the topology of the mesh is updated with the insertion of a new surface with the algorithm described in [16].

The value of the normal strength $\sigma_c(N)$ is then adopted to define the cohesive properties of the cohesive surface newly inserted. The corresponding anisotropic cohesive law is characterized by a scaling dependent on the direction of the axis, see Figure 2.

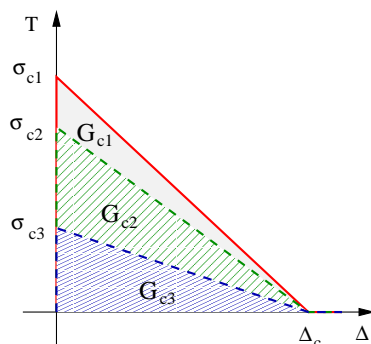


Figure 2: Set of cohesive laws considered in the present model. Both cohesive strengths and critical energy release rates are scaling proportionally. The maximum opening displacement Δ_c does not change with the orientation.

3 NUMERICAL RESULTS

Numerical analyses of arterial dissection have been carried out by using a finite element code equipped with explicit fracture algorithm, able to deal with anisotropic materials and anisotropic cohesive resistance according to the previous definitions [17].

The experimental results presented in [8], concerning a program of dissection tests on media layer of human arteries, are the basis of the present study. Finite element simulations of the experiments have been presented by Gasser *et al.* [18] by using the X-fem approach and a transversally isotropic cohesive model. The numerical simulations in [18] have been replicated here, considering an equal length, equal cross area specimen, and adopting the same material properties, in order to provide a reference analysis.

The material properties adopted in the reference simulation are listed in Table 1 [18].

Table 1: Elastic and cohesive material properties for the two-fiber reinforced material adopted in the simulation of the dissection in the aortic media.

K (kPa)	μ (kPa)	k_1 (kPa)	k_2 (-)	γ ($^\circ$)	G_c (N/mm)	T_c (kPa)
1.66	0.0162	0.0981	10	5	0.049	140

The specimen of human media is a rectangular strip 4.0 mm long, 0.6 mm wide, and 0.15 mm thick, with 0.2 mm precrack. Plane strain conditions are assumed. The specimen is fully constrained on the right side, while the two arms at the left side are pulled apart by applying a transversal

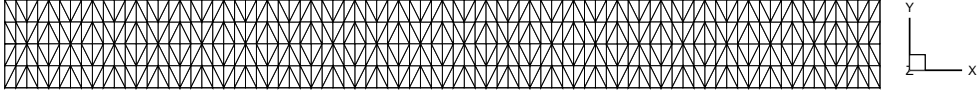


Figure 3: Finite element mesh adopted for the reference analysis of dissection in an aortic media.

displacement normal to the strip axis. The displacement, 4 mm, is imposed at all the nodes belonging to the free end of each arm, and is applied through small quasi-static increments.

The mesh adopted for the reference analysis is reported in Fig. 3. It consists of 2529 nodes and 996 tetrahedral elements. The mesh size is $h = 0.025$ mm (fine mesh). Fig. 4(a) shows the final configuration of the reference specimen. The applied displacement does not cause the full opening of the specimen.

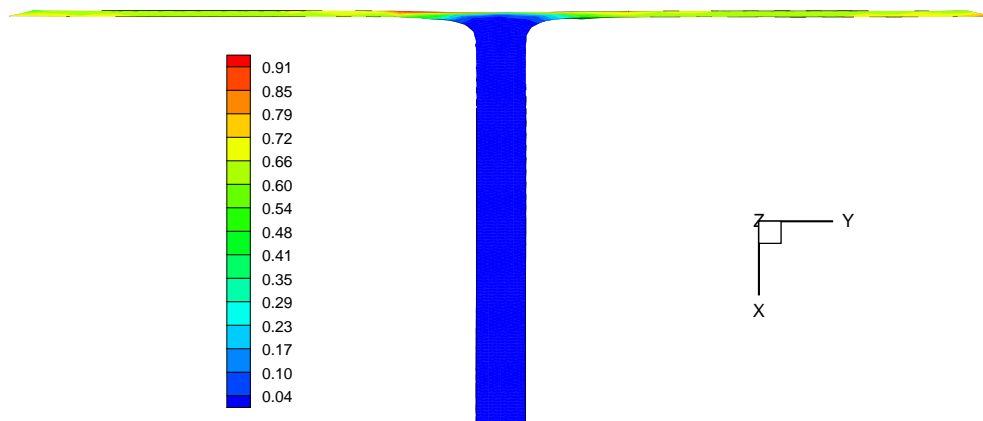
To evaluate the sensitivity of the numerical model to the mesh size, two additional calculations have been carried out, with $h = 0.05$ mm (medium mesh) and $h = 0.1$ mm (coarse mesh). The comparison is done in terms of pulling force, i.e. the numerical value of the nodal reactions divided by the specimen width, versus the total separation of the two arms, see Fig. 5. It is evident the mesh dependency of the model. In fact, the coarse mesh is not able to resolve the cohesive zone and the average stress on the interface surface does not satisfy the fracturing condition (10). The medium and the fine meshes are able to capture a response which in the average is close to the experimental value reported in [8], 23 N/m, with a very nice correspondence for the fine mesh.

The way the cracks propagate depends mainly on the cohesive properties, i.e. the cohesive strength and the fracture energy. The sensitivity of the model to the cohesive traction has been investigated through a second set of numerical analyses with constant fracture energy $G_c = 0.049$ N/mm. The chosen values for the cohesive strength are reported in Table 2, together with the maximum and the average pulling force obtained from the numerical calculations. Fig. 6 reports the plots of the force/width versus displacement gap. It is evident that a smaller cohesive strength provides a smaller average pulling force. The reduced pulling forces correspond to a reduced stretching and thinning of the specimen, see Fig. 4(b) for the case $T_c = 14.01$ kPa.

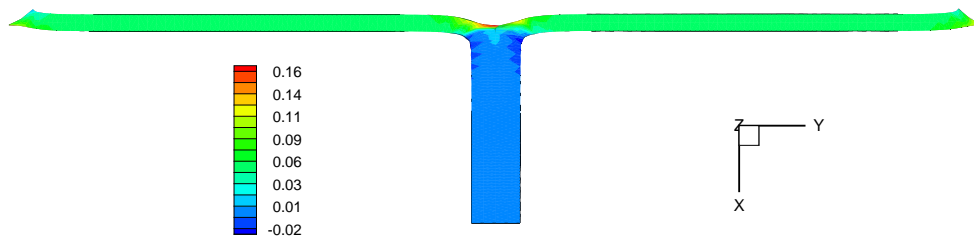
The influence of energy fracture on the fracture initiation has been investigated by reducing the

Table 2: Effects of the cohesive strength T_c on the average force/width response of the dissection.

	T_c (kPa)	Force/Width (mN/mm)	
		max value	average value
(a)	14.01	6.09	5.20
(b)	56.04	12.38	10.32
(c)	112.08	19.98	16.00
(d)	140.01	23.95	18.45
(e)	168.12	28.11	20.70



(a)



(b)

Figure 4: Deformed configurations of the aorta specimen after the application of the whole displacement. Contour levels refer to the Cauchy stress component in the vertical direction, expressed in MPa. (a) Reference case, $T_c = 140$ kPa. (b) Alternative case with reduced cohesive strength $T_c = 14$ kPa.

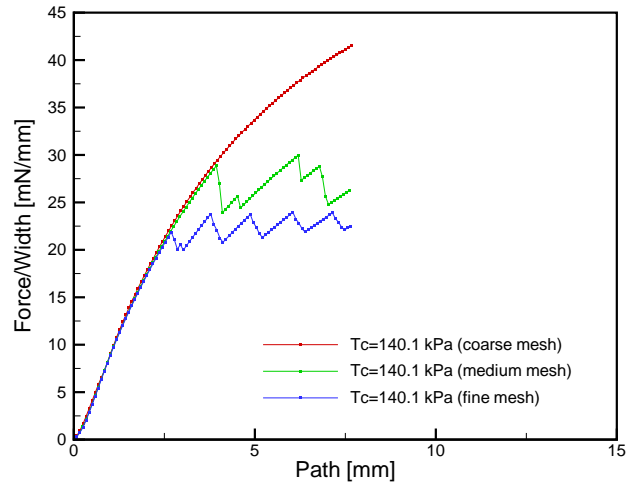


Figure 5: Force/width versus gap displacement in the numerical analyses of the media dissection. Effects of the mesh size ($T_c = 140.1$ kPa).

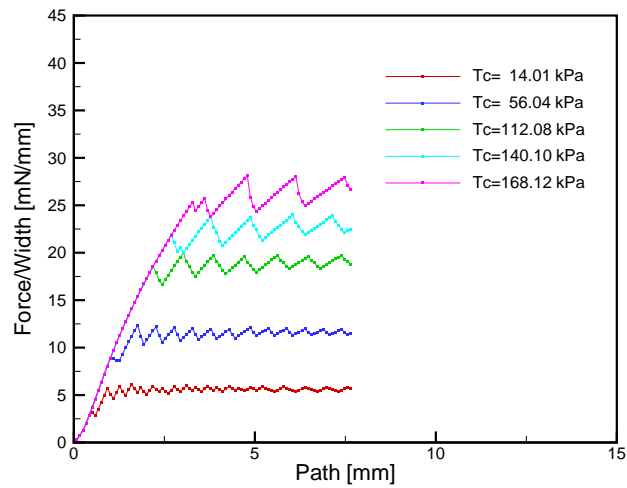


Figure 6: Force/width versus gap displacement in the numerical analyses of the media dissection. Effects of the cohesive strength (fine mesh).

cohesive energy from 1.4 N/mm [19] to 0.16 N/mm [3]. No remarkable differences on the crack initiation and peeling force have been observed with respect to the reference cases.

4 CONCLUSIONS

A recently developed finite element model of anisotropic fragmentation, based on cohesive theories [17], has been applied to the analysis of dissection of the media layer of a human artery. A program of numerical analysis have been performed with the aim to investigate the influence of the mesh discretization and of cohesive parameters on the separation process. Additional sensitivity analyses are needed, which involve the elastic constants of the model and the microstructure of the reinforcing fibers. In particular, it would be interesting to explore the effects of the fiber orientation and dispersion. This study represents a contribution to the development of a reliable model of the human artery able to describe important damaging events like plaque ruptures and intramedial dissections.

References

- [1] Svensson L.G. and Crawford, E.S., "Aortic dissection and aortic aneurysm surgery, II: clinical observations, experimental investigations, and statistical analyses," *Curr. Probl.Surg.*, **29**, 9151057 (1992).
- [2] Tam, A.S.M., Sapp M.C. and Roach, M.R., "The effect of tear depth on the propagation of aortic dissections in isolated porcine thoracic aorta," *Journal of Biomechanics*, **31**, 673676 (1998).
- [3] Carson, M.W. and Roach, M.R., "The strength of the aorta media and its role in the propagation of aortic dissection," *Journal of Biomechanics*, **23**, 579588 (1990).
- [4] Wolinsky, H. and Glagov, S., "Structural basis for the static mechanical properties of the aortic media," *Circulation Research*, **14**, 400413 (1964).
- [5] van Baardwijk, C. and Roach, M.R., "Factors in the propagation of aortic dissections in canine thoracic aortas," *Journal of Biomechanics*, **20**, 6773 (1987).
- [6] MacLean, N., Dudek, F.N.L. and Roach, M.R., "The role of radial elastic properties in the development of aortic dissections," *Journal of Vascular Surgery*, **29**, 703710 (1999).
- [7] Patel, D.J., Janicki, J.S., Vaishnav, R.N. and Youg, J.T., "Dynamic anisotropic viscoelastic properties of the aorta in living dogs," *Circulation Research.*, **32**, 93107 (1973).
- [8] Holzapfel, G.A. and Sommer, G., "Dissection properties of the human aortic media: an experimental study," *Journal of Biomechanical Engineering*, **130**, 1-12 (2008).
- [9] Holzapfel, G.A., Gasser, T.C. and Ogden, R.W., "A new constitutive framework for arterial wall mechanics and a comparative study of material models," *Journal of Elasticity.*, **61**, 1-48 (2000).
- [10] Spencer, A.J.M., *Deformation of fiber-reinforced materials*, Oxford University Press, Oxford (1982).
- [11] Wells, G.N., de Borst, R. and Sluys, L.J., "A consistent geometrically non-linear approach for delamination," *Int. J. Numer. Meth. Engng.*, **54**, 1333-1355 (2002).

- [12] Gasser, T.C. and Holzapfel, G.A., "Geometrically non-linear and consistently linearized embedded strong discontinuity models for 3D problems with an application to the dissection analysis of soft biological tissues," *Computer Methods in Applied Mechanics and Engineering*, **192**, 5059-5098 (2003).
- [13] Yu, C., Pandolfi, A., Ortiz, M., Coker, D. and Rosakis, A.J., "Three-dimensional modeling of intersonic crack-growth in asymmetrically loaded unidirectional composite plates," *International Journal of Solids and Structures*, **39**, 6135-6157 (2002).
- [14] Greco, F. and Lonetti, P., "Mixed mode dynamic delamination in fiber reinforced composites," *Composites: Part B*, **40**, 379392 (2009).
- [15] Ortiz, M. and Pandolfi, A., "Finite-deformation irreversible cohesive elements for three-dimensional crack propagation analysis," *International Journal for Numerical Methods in Engineering*, **44**, 1267-1282 (1999).
- [16] Pandolfi, A. and Ortiz, M., "An efficient adaptive procedure for three-dimensional fragmentation simulations," *Engineering with Computers*, **28**, 148-159 (2002).
- [17] Ferrara, A. and Pandolfi, A., "Numerical modelling of fracture of human arteries," *Computer Methods in Biomechanics and Biomedical Engineering*, **11**, 553567 (2008).
- [18] Gasser, T. and Holzapfel, G.A., "Modeling the propagation of arterial dissection," *European Journal of Mechanics A/Solids*, **25**, 617633 (2006).
- [19] Purslow P., "Positional variations in fracture toughness, stiffness and strength of descending thoracic pig aorta," *Journal of Biomechanics*, **16**, 947955 (1983).